Aggregation in Water of Dextran Hydrophobically Modified with Bile Acids

Marieta Nichifor,[†,‡] António Lopes,[†] Adrian Carpov,[‡] and Eurico Melo*[,†,§]

Instituto de Tecnologia Química e Biológica, OEIRAS, Portugal, Institute of Macromolecular Chemistry "Petru Poni" IASSY, Romania, and Instituto Superior Técnico, LISBOA, Portugal

Received March 19, 1999; Revised Manuscript Received July 13, 1999

ABSTRACT: The intra- and/or intermolecular aggregation and the structure of the aggregates formed in water by hydrophobically modified dextrans, prepared by covalent attachment of cholic or deoxycholic acid to dextran of $M_v = 30\,000$, were investigated by various fluorescence and light scattering techniques. From the variation of the fluorescence quantum yield and fluorescence emission maximum of a hydrophobic fluorescent probe, *N*-phenyl-1-naphthylamine, with polymer concentration, we conclude about the value of the critical aggregation concentration, cac, and the existence of intermolecular aggregation below cac. The values of cac are found to depend on the nature of the hydrophobic moiety and the degree of substitution. The hydrodynamic radii of the aggregates are determined using dynamic light scattering, and the apparent weight-average molecular weights, radii of gyration, and second virial coefficients are evaluated by static light scattering over a very large concentration range. The results show that below a given critical concentration the hydrophobically modified dextrans form big and loose aggregates and small and compact ones at concentrations higher than 0.2 g %. A transition between the two types of aggregates begins at 0.02 g %, the concentration that we keep calling cac despite the fact that it is the concentration at which the formation of compact aggregates begins rather than that for which intermolecular aggregation occurs. The results are compared with those for unmodified dextran for which no aggregation was observed.

Introduction

Amphiphilic polymers have been extensively studied for theoretical reasons and for their wide range of applications in oil recovery, latex paint technology, biotechnology, or medicine.[1−3] Many of them are water-soluble polymers substituted with hydrophobic or amphiphilic side groups such as alkyl, aralkyl, and cycloalkyl[4−8] or steroids such as cholesterol[9−12] and deoxycholic acid.[13] When dissolved in water, amphiphilic polymers can self-aggregate due to intra- and/or intermolecular hydrophobic interactions.[2−4] By analogy with the phenomena of micelle formation of small surfactants or lipids, aggregation of amphiphilic polymers is controlled by the balance between the interaction of the hydrophobic moieties and that of the hydrophilic chains. The concentration at which polymer aggregation starts is usually called the critical aggregation concentration, cac. Many different techniques, including viscometry,[5,7,14] fluorescence,[4−6,9−13] light scattering,[6,9,11,13] or NMR measurements,[6] have been used to detect the aggregates and characterize the structures formed.

Bile acids are natural products consisting of a facially amphiphilic steroid nucleus with a hydrophobic β-side and a hydrophilic α-side.[15,16] When these compounds are part of a water-soluble polymer, the resulting amphiphilic polymer might exhibit a better compatibility with biological systems and interact favorably with proteins, enzymes, or lipids.[2,15,17]

To obtain amphiphilic polymers with possible application in biotechnology and medicine, bile acid modified dextrans (BAMDex) were synthesized by covalent attachment of cholic acid or deoxycholic acid to dextran through ester links. The chemical structure of the obtained BAMDex is depicted in Scheme 1. The presence of aggregates and their structure formed in BAMDex−water solutions is here investigated using a combination of fluorescence techniques and static and dynamic light scattering.

For detection of the polymer cac values we use the well-established method of *N*-phenyl-1-naphthylamine (NPN) fluorescence quantum yield and emission maximum.[9,18] The method is based on the large increase in the fluorescence quantum yield and strong bathochromic shift of the fluorescence emission observed when the solvent surrounding the hydrophobic deprotonated NPN ($pK_a \cong 5.5$) becomes more polar or viscous.[18]

Steady-state fluorescence anisotropy is employed to evaluate the microviscosity of the environment of NPN by using the Perrin formalism that, for a given chromophore, relates the emission anisotropy with the viscosity of its environment, η, and the emission lifetime, τ.[19]

On the basis of the sensitivity of the steady-state fluorescence anisotropy to the viscosity of the environment,[20] we have attempted to determine the partition constant, K_p, of NPN between the polymer microdispersed phase and the bulk. The method presumes an equilibrium between two phases of known fractional volume, where the fluorescence anisotropy of the fluorophore, in this case NPN, is quite different. As will be shown in the Results section, with these polymers the interpretation of the data is not straightforward.

Static light scattering (SLS) data allow the evaluation of the weight-average molecular weight, M_w, the radius of gyration, R_g, and the second virial coefficient A_2 of the polymer aggregates present in dilute solutions.[21] In this way these aggregates have been characterized, namely the number of single macromolecules (unimers)

† Instituto de Tecnologia Química e Biológica.
‡ Institute of Macromolecular Chemistry "Petru Poni" IASSY.
§ Instituto Superior Técnico.
* Correspondening author: ITQB, Apartado 127, P-2781-901 OEIRAS, Portugal. e-mail: eurico@itqb.unl.pt.

10.1021/ma990408k CCC: $18.00
Published on Web 10/01/1999

Scheme 1

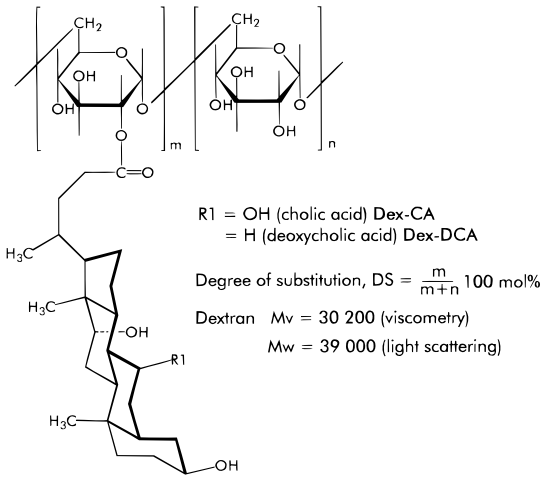

associated could be evaluated, as a function of the polymer concentration and polymer characteristics.[22] In addition, from the second virial coefficient we determine the concentration ranges for which polymer−polymer interactions are thermodynamically favored and those for which interactions of polymer with solvent prevail.

Particle size (hydrodynamic radii) and particle size distribution are determined by dynamic light scattering (DLS), for several concentrations of each polymer.[22] Comparison of the radius of gyration, R_g, obtained from SLS, with the hydrodynamic radius, R_h, from DLS, reveals the geometry of the macromolecular aggregate based on the well-known R_g/R_h relations. For extended chains (cylinders) $R_g/R_h \geq 2$,[23] for flexible random coils R_g/R_h is 1.5−1.8 in a good solvent[23,24] and 1.3 in a Θ solvent,[23] and for compact spheres it takes values of about 0.775.[25]

Materials and Methods

Reagents and Solvents. *Synthesis of bile acid modified dextran (BAMDex)* was described in detail elsewhere.[26] Briefly, polymers with the structure presented in Scheme 1 were obtained by reacting dextran (M_w = 30 200, M_w/M_n = 1.112) with a bile acid in the presence of *N*,*N*-dicyclohexylcarbodiimide as a coupling agent and 4-(*N*,*N*-dimethylamino)pyridine as a catalyst. Dextran modified with cholic acid (Dex-CA) or deoxycholic acid (Dex-DCA) with degrees of substitution (DS) of 2−6 mol % (moles of bile acid bound/100 glucopyranosidic structural units) were used for fluorescence and light scattering measurements. For all solutions, solvent mixtures, and suspensions a phosphate buffer of pH = 7.0, 0.01 M in Na^+ in Elgastat water, was used. All the other solvents used were spectroscopic or HPLC grade from Merck (Germany). The fluorophore *N*-phenyl-1-naphthylamine (NPN) was from Sigma and was recrystallized twice from ethanol.

Solutions were made by dilution of a 2 g % (g/dL) polymer stock solution in buffer prepared by 10−15 min bath sonication. Solutions of different concentrations in BAMDex, containing 1.0×10^{-6} M of *N*-phenyl-1-naphthylamine (NPN), were obtained by vortexing the BAMDex solutions of adequate concentration in vials where a film of NPN was deposited by solvent evaporation. The maximum concentration used in both fluorescence and light scattering measurements was 2 g %, much lower than the critical overlap concentration c^* = 5−10 g % (calculated as $1/[\eta]$, where $[\eta]$ is the intrinsic viscosity of polymer in water, 0.1−0.2 cP^{-1}).[14,26,27]

Methods. All the fluorometric measurements where done at a temperature of 25 ± 1 °C, except those with PEG 600 done at 30 °C and the LS at 25 ± 0.1 °C.

Steady-State Fluorometric Measurements. Steady-state fluorescence spectra and fluorescence anisotropy values were obtained using a SPEX Fluorolog 212 in L conformation. Excitation wavelength was 340 nm, and the fluorescence emission always corrected for instrumental response. In the case of the fluorescence anisotropy the instrumental correction factor, $G = I_{HV}/I_{HH}$, was determined by the method of Azumi and McGlynn.[28] Fluorescence intensity of NPN emission in 1,4-dioxane/water mixtures was corrected for solution refractive index.

Time-Resolved Fluorometric Measurements. Fluorescence lifetimes of NPN in the absence and presence of BAMDex were performed using the single photon counting technique. Equipment used and deconvolution methods have been described elsewhere.[29]

Light Scattering Measurements. The light scattering measurements were performed with an apparatus from Brookhaven Instruments, Inc., model 2030AT, equipped with a He−Ne laser (632.8 nm) and a 136-channel autocorrelator. The sample solutions were filtered directly into cylindrical cells through membrane filters (nominal pore size 0.45 μm, SRI) and then centrifuged at approximately 1300 g for 45 min to remove dust particles. For DLS measurements the scattering angle was fixed at 90° and varied from 35° to 145° in the case of SLS measurements. The d*n*/d*c* values were determined with a differential refractometer (G. M. Wood RF600), being equal to 0.150 mL/g for all polymers under study. Each Zimm plot was made with a minimum of seven logarithmically spaced concentrations. Because of the low concentration range in which we are working, all the solutions had a transmitance higher than 0.95, convenient for the light scattering measurements,[30] and are much below the critical overlap concentration, c^*, which for these polymers is about 5−10 g % as previously stated. The use of a concentration much lower than c^* is usually accepted as a condition for not being too far from the validity range of Rayleigh−Gans−Debye theory for light scattering.[22]

Hydrodynamic diameter, D_h, distributions (histograms) were obtained with a CONTIN routine, and the value we refer to as R_h is the mean value of the radii distribution.

Data Analysis. *Microviscosity of NPN Environment by Steady-State Fluorescence Anisotropy.* If NPN is considered as a roughly spherical molecule of molar hydrodynamic volume V_h rotating freely in a medium of viscosity η, at a given temperature, *T*, the viscosity of the medium is related to the fluorescence anisotropy, *r*, and to the fluorescence lifetime of the molecule, by the Perrin equation

$$\frac{1}{\eta} = \frac{V_h r_0}{RT}\frac{1}{\tau}\left(\frac{1}{r} - \frac{1}{r_0}\right) \tag{1}$$

where r_0 is the limiting anisotropy in rigid media. The experimental value of $r_0 = 0.17 \pm 0.03$ was obtained from a Perrin plot for PEG 600/acetone mixtures, and this value was confirmed by measuring the fluorescence anisotropy in a organic glass of methylcyclohexane at 77 K. The fluorescence lifetimes of NPN in both polymers are well fitted by a biexponential law with times τ_1 and τ_2 and preexponentials a_1 and a_2, respectively. The average lifetime, $\langle\tau\rangle$, used for the microviscosity calculation with eq 1, was obtained in the usual way, according to eq 2.

$$\langle\tau\rangle = \sum_i a_i\tau_i^2 / \sum_i a_i\tau_i \tag{2}$$

Aggregate/Water Partition Constants by Fluorescence Anisotropy. The total fluorescence anisotropy measured, *r*, relates to K_p, according to eq 3:[31]

$$r = \frac{r_w + x_{agg}\gamma\xi K_p r_{agg}/(1 - x_{agg})}{1 + x_{agg}\gamma\xi K_p/(1 - x_{agg})} \tag{3}$$

where r_w is the fluorescence anisotropy of the probe in water, r_{agg} the fluorescence anisotropy in the aggregate, and both $\xi = \epsilon_{agg}\Phi_{agg}/\epsilon_w\Phi_w$ and γ, correction factors for the relative intensity of fluorescence at the wavelength where the emission

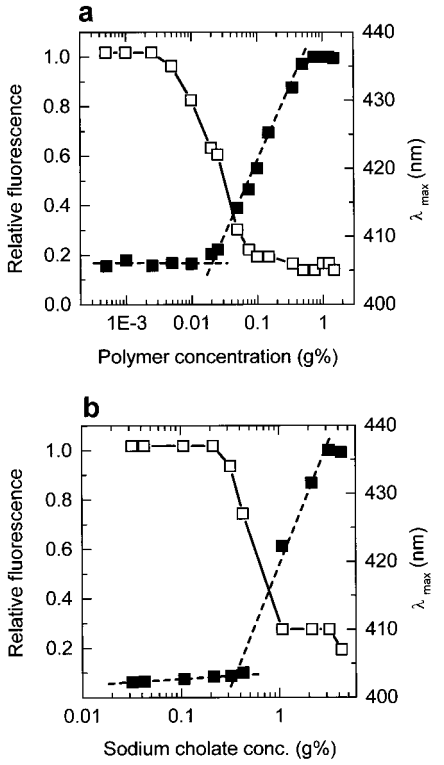

Figure 1. Relative fluorescence emission intensity (■) and maximum of fluorescence emission (□) of NPN as a function of (a) Dex-CA (DS = 4.0 mol %) concentration in buffer solution and (b) sodium cholate concentration in water. The straight lines over the fluorescence intensity data are an attempt to define the cac of the polymer and the cmc of cholate.

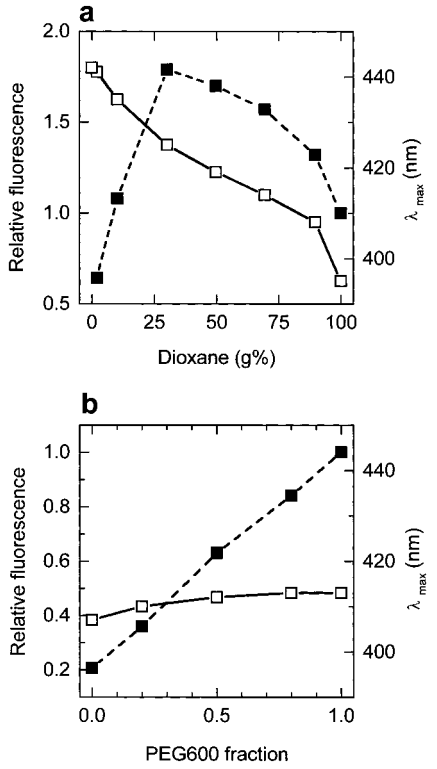

Figure 2. Relative quantum yield (■) and fluorescence maximum (□) of NPN in **(**a**)** 1,4-dioxane/water mixtures as a function of dioxane concentration in g% and **(b)** PEG 600/acetone mixtures as a function of PEG 600 concentration in g%. Curves do not correspond to any model.

is observed. Measuring r for different polymer concentrations, each corresponding to a fractional volume occupied by the aggregate pseudophase, $x_{agg} = V_M c$ where V_M is the polymer molar volume and c the concentration; K_p and the fluorescence anisotropy in the aggregate, r_{agg}, are obtained.

Weight-average molecular weight, M_w, radius of gyration, R_g, and second virial coefficient, A_2, were calculated by the usual Zimm method based on the Rayleigh−Gans−Debye theory for light scattering. According to the theory, the variation of the relative intensity of scattered light, I_s/I_0, with the observation angle, θ (Rayleigh factor, $R_\theta = [d^2(I_s/I_0)]/\sin^2\theta$), is related to M_w, R_g, and A_2, for a given concentration, c, through eq 4.

$$\frac{Kc}{R_\theta} \cong \frac{1}{M_w}\left(1 + \frac{16\pi^2 n_0^2}{3\lambda_0^2} R_g^2 \sin^2\frac{\theta}{2}\right) + 2A_2 c \qquad (4)$$

In this equation the optical constant $K = [4\pi^2 n_0^2 (dn/dc)^2]/N_A\lambda^4$, where n_0 and n are respectively the refractive index of the solvent and solution.

Results and Discussion

Transition Energy and Quantum Yield of the Fluorescence Emission of NPN in the Presence of BAMDex. In Figure 1a the relative fluorescence emission intensity of NPN is presented as a function of Dex-CA (DS = 4.0 mol %) concentration. The fluorescence quantum yield is nearly constant until about 0.02 g % of polymer, increases rapidly above this concentration, and reaches the maximum at about 0.8 g %. In the same figure the fluorescence emission maximum of NPN as a function of polymer concentration is also presented. A steady decrease of the fluorescence maximum from about 0.002 g % until around 0.8 g % is observed, which reflects also a change in polarity and/or viscosity of the average environment of NPN. The large hypsochromic shift observed for concentrations much lower than 0.02 g % conflicts with the constancy of the fluorescence quantum yield in the same concentration range. Moreover, the sudden increase of fluorescence intensity at about 0.02 g %, in principle interpreted as the cac of the polymer, is not mirrored in the emission maximum shift.

When the same method is used for the determination of the cmc of cholic acid sodium salt, there is no evidence for a significant difference between the values obtained from fluorescence intensity and fluorescence emission maximum, both giving about 0.3 g % as expected[18] (Figure 1b). To explain the results obtained with the polymer solution, further understanding of the photophysical behavior of NPN is needed.

In Figure 2a we present the variation of the relative quantum yield and fluorescence maximum of NPN in 1,4-dioxane/water mixtures as a function of dioxane concentration. While the emission maximum decreases steadily with the increase of dioxane concentration, the fluorescence quantum yield reaches a maximum for ca. 25 g % dioxane. In view of these results, we conclude that, if a hypsochromic shift undoubtedly indicates an increase in the hydrophobicity of the average environment of NPN, the quantum yield does not correlate in a simple manner with the characteristics of the solvent.

The unchanged quantum yield between 0.002 and 0.02 g % polymer concentration does not mean that the average environment of the probe remains unchanged, as long as a change in emission maximum is noted. Perhaps the fluorescence quantum yields in the different environments where the chromophore molecules resides average to approximately the same value when changing the polymer concentration. In fact, in this

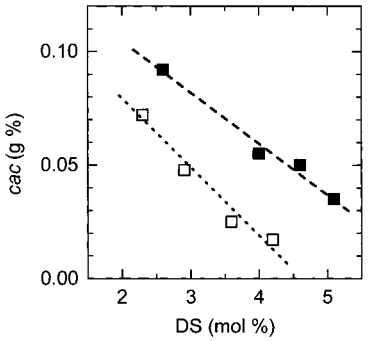

Figure 3. Values of the cac obtained as described in the text as a function of the degree of substitution of the polymer for Dex-CA (□) and Dex DCA (■).

concentration range the shape of the spectra (but not the intensity) can be simulated as a composition of spectra in 0.005 and 1 g % (data not shown).

The sharp increase of quantum yield for Dex-CA concentration higher than 0.02 g % is probably due to a new type of aggregates where NPN is now trapped. The vicinity of NPN in these aggregates is certainly more hydrophobic, as we conclude from the shift in the fluorescence maximum, but the 5-fold increase in the quantum yield cannot be simply explained in terms of polarity. In Figure 2b the variation of NPN emission maximum and quantum yield in a mixture of PEG 600/acetone as a function of PEG 600 weight concentration shows that for a nearly constant transition energy the quantum yield of NPN increases with viscosity. Therefore, the large increase in quantum yield for high concentration of Dex-CA is due to both the more hydrophobic and more viscous environment of the NPN. In this way we can, in principle, ascribe the inflection in the quantum yield versus concentration curve to the appearance of a more compact type of polymer aggregation and define this concentration as the cac of the polymer. Below the cac, the hydrophobic parts of polymer may partially protect NPN from contact with water, resulting in the observed shift of fluorescence emission maximum.

It is also to be noted that we are never observing NPN dissolved in water. In fact, the fluorescence emission maximum for concentrations lower than 0.002 g % reveals interaction of NPN with an environment with lower polarity than that of the pH = 7.0 buffer. Besides, it is not believable that the fluorescence quantum yield of NPN interacting with the polymer, even if in a loose coil aggregate, is the same as in water, what would be necessary for the constancy in fluorescence intensity. With the present data it cannot be discarded the possibility that NPN itself can induce aggregation, namely aggregation of bile acid moieties around its molecules.

Variation of NPN fluorescence quantum yield and emission maximum with concentration is similar for all BAMDex investigated. However, the concentration corresponding to the inflection of the fluorescence intensity−concentration curve, cac, depends on the type of bile acid bound and also on the DS of the polymer. For the same degree of substitution the cac is lower for polymers modified with deoxycholic acid, and for the same substituent it decreases with the increase of the degree of substitution as shown in Figure 3. Both findings are easily understandable in terms of the higher polymer hydrophobicity conferred by DCA as well as that resulting from a higher degree of substitution.

Table 1. Fluorescence Lifetime Components, τ_i, and Corresponding Amplitudes, a_i, and Average Fluorescence Lifetime, $\langle\tau\rangle$, of NPN in Solutions with 1 g % of Polymer in Buffer Solution; for the Same Polymer Concentration the Fluorescence Anisotropy, r_{agg}, Is Also Presented

	lifetimes/amplitude			
polymer	τ_1 (ns)/a_1	τ_2 (ns)/a_2	$\langle\tau\rangle$ (ns)	r_{agg}
Dex-CA (DS = 4.0%)	9.03/0.40	24.0/0.60	21.0	0.11
Dex-DCA (DS = 3.6%)	6.27/0.40	19.9/0.60	17.6	0.13

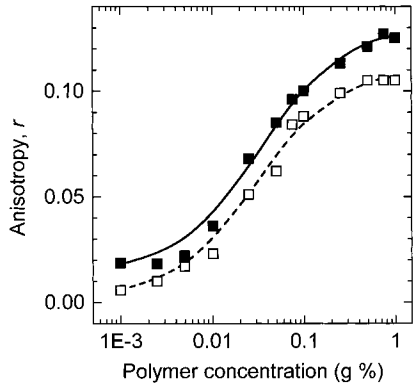

Figure 4. Variation of the steady-state fluorescence anisotropy of NPN as a function of Dex-CA (DS = 4.0%) (□) and Dex-DCA (DS = 3.6%) (■) concentration. The curves were obtained from the fit of eq 2 to the experimental data with $K_p = 500$.

Fluorescence Anisotropy of NPN in the Presence of BAMDex. Fluorescence anisotropy, r_{agg}, and average lifetimes of NPN in solutions with a high concentration, 1 g %, of dextran modified with cholic or deoxycholic acid are presented in Table 1. These fluorescence anisotropies are to be compared with the anisotropy in rigid media, $r_0 = 0.17 \pm 0.03$.

For this polymer concentration all NPN resides in the polymer, and the fluorescence anisotropy is a measure of the chromophore rotation during its fluorescence lifetime, the correlation time for the rotation of the aggregate itself in water being expected to be much larger than the lifetime of the probe. According to eq 1, and using a hydrodynamic radius of NPN equal to 0.6 nm, we obtain a viscosity of the environment of NPN of ca. 1.7 P in Dex-CA, and 2.5 P in Dex-DCA, which indicates a very high viscosity for the region where NPN resides. The anisotropy values themselves are not easy to compare with other values from the literature. For example, the *r* values of 0.3 reported for deoxycholic acid modified chitosan[13] exceed our r_0 value which may be due to different excitation and emission wavelength or other technical differences.

The variation of fluorescence anisotropy, *r*, of NPN with polymer concentration in buffer solutions of Dex-CA (DS = 4.0%) and Dex-DCA (DS = 3.6%) (Figure 4) shows a constant increase in the fluorescence anisotropy as a result of the change in the average environment of the probe with a small discontinuity at 0.02 g %, which may have the same origin of the inflection point found in Figure 1. The curves in Figure 4, obtained from the fit of the experimental data to a hypothetical partition between water and polymer aggregate for a partition constant $K_P = 500$ determined with eq 3, do not describe adequately the data. At the first sight it seems that, despite a possible change of the aggregate characteristics, the affinity of NPN for the polymer is the same, whatever the concentration. However, this simple rea-

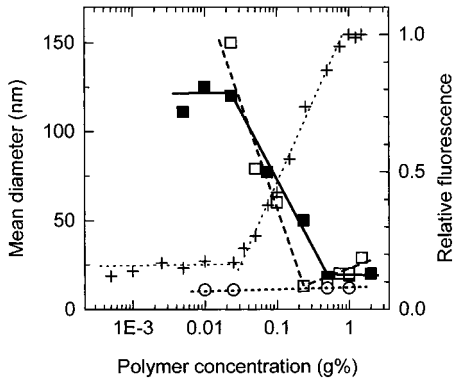

Figure 5. Hydrodynamic radius of dextran (○), Dex-CA (DS = 4.0 mol %) (□), and Dex-DCA (DS = 3.6 mol %) (■) as a function of polymer concentration obtained by dynamic light scattering. The fluorescence intensity of NPN in Dex-DCA (DS = 3.6 mol %) (+) is also presented for comparison purposes.

soning is most probably erroneous because the fluorescence anisotropy of NPN is different for different types of aggregates, and we are certainly measuring the partitioning between two types of aggregates, formed from extended coils at low concentration and tight coils for the high concentration range. If this is the case, the value of K_P obtained is devoid of physical meaning, and at this stage, it is not possible to determine the partition constant between aggregates because of the continuous variation of the properties of the aggregates and the unknown relative volume fraction they represent. The approximate fit is not surprising because the shapes of the curve in any case should be similar.

Whatever the degree of substitution for each type of BAMDex, the fluorescence anisotropy of NPN tends to the same value (r_{agg} listed in Table 1) at high polymer concentrations. The affinity for the polymer, however, depends on the DS being higher for higher DS. For the lower values of DS the fit of the experimental data to eq 3 is even worse than that presented in Figure 4 (data not presented), showing more clearly two different regimes, one for low and the other for high concentrations.

Dynamic Light Scattering of BAMDex Aqueous Solutions. In Figure 5 the hydrodynamic diameters obtained by DLS for original dextran or dextran modified with CA (DS = 4.0 mol %) and DCA (DS = 3.6 mol %) as a function of polymer concentration are presented. While the R_h of the unmodified polymer does not change with concentration, a large variation is observed for both Dex-CA and Dex-DCA. This variation is mirrored by that of fluorescence intensity of NPN in polymer solution (the data for a Dex-CA with a DS = 4.0 mol % are also included in the figure for comparison purposes). Considering the rather low molecular weight of these polymers, the very large R_h obtained for the modified dextrans in the low concentration range, when compared with that for the nonmodified polymer, may be assigned to the interaction between the hydrophobic moieties of different polymer chains, resulting in the formation of large and loose aggregates. This result corroborates the interpretation given for the NPN fluorescence data.

For polymer concentrations larger than cac the R_h values of the modified polymers decrease continuously until about 10 nm, remaining approximately constant for concentrations larger than 0.2−0.5 g %. This radius is twice that obtained for the unmodified dextran. At these large concentrations the aggregates should be very compact, in accordance with the high local viscosity and low polarity revealed by the fluorescence methods. It is important to note that we use here the concept of cac quite liberally because in fact we are referring not to the aggregation but to a compaction and reduction of the number of polymer molecules per aggregate, as will become even more clear after presentation of the SLS results.

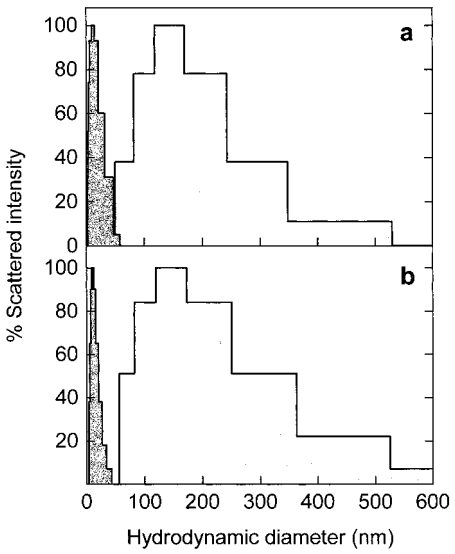

Figure 6. Histogram of hydrodynamic diameters obtained from DLS for **(**a**)** Dex-CA (DS = 4.0%) at 0.025 g% (light shade) and 0.5 g% (dark shade) and **(**b**)** Dex-DCA (DS = 3.6%) at 0.025 g% (light shade) and 0.25 g% (dark shade).

The distribution of hydrodynamic diameters for Dex-CA (DS = 4.0%) and Dex-DCA (DS = 3.6%) is presented in Figure 6. In both cases the distribution is narrow for the high concentration regime and very broad for the low concentrations. The diversity of aggregates existing in the low concentration range may justify the constancy of the average fluorescence quantum yield observed. In the transition region the R_h distribution is extremely broad, and it is difficult to say whether there is a bimodal size distribution as expected, but at the end of the transition region a bimodal distribution is clearly obtained for both polymers (Figure 7).

Static Light Scattering of BAMDex Aqueous Solutions. We have obtained reliable Zimm plots in the concentration ranges where both relative fluorescence intensity and R_h values are approximately constant. In Figure 8 we show those obtained for dextran, c = 0.6−2.0 g%, Dex-DCA (3.6 mol %), c = 0.002−0.02 g%, and Dex-DCA (3.6 mol %), c = 0.6−2.0 g %. In Table 2 the apparent weight-average molecular weight, the second virial coefficient, and the radius of gyration, R_g, obtained from the Zimm plots for dextran and both modified Dex-CA and Dex-DCA in the range of concentrations under study are presented. The M_w obtained from extrapolation to $c = 0$ and $\theta = 0$ do not differ in any case more than 1%, but the physical meaning of R_g in this way obtained may be questioned.[12] Thus, the presented R_g's are not intended to be taken as absolute values, but they are useful for comparison purposes.

For the case of the unmodified dextran R_g does not present a large change with polymer concentration, a behavior already observed for R_h. Moreover, the apparent molecular weights are, within the error, equal to those specified for the molecular weight determined by

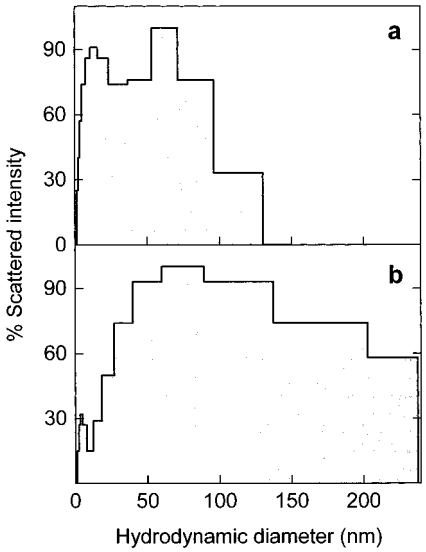

Figure 7. Histogram of hydrodynamic diameter distribution for the intermediate concentration range. Solutions with 0.1 g % **(**a**)** Dex-CA (4.0 mol %) and **(**b**)** Dex-DCA (3.6 mol %).

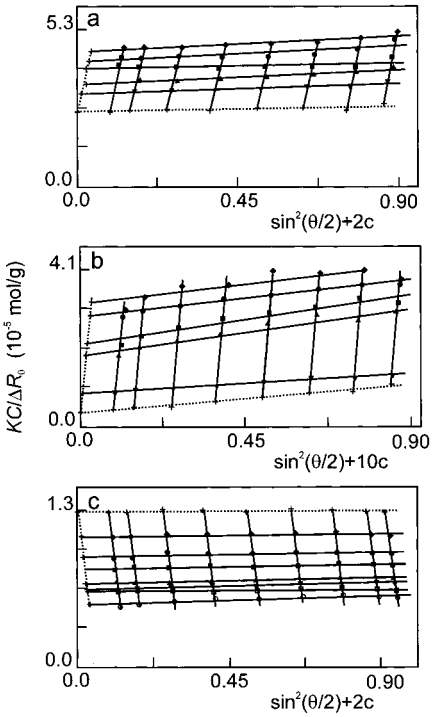

Figure 8. Zimm plots for **(**a**)** dextran, $c = 0.6-2.0$ g % and two ranges of concentrations of Dex-DCA (3.6 mol %), c, in the high- and low-concentration regions: **(**b**)** $c = 0.002-0.02$ g % and **(**c**)** $c = 0.6-2.0$ g %.

viscometry ($M_v = 30\,000$), which indicates the presence of polymer as a unimer. The ratio $R_g/R_h > 2$ indicates a very extended chain which is coherent with a persistent length of dextran of 5−10 monomer units, indicating that for molecular weights around 30−40 kDa the conformation of the molecule should be a rather extended random coil.[32] Below the cac (dilute regime) the high apparent M_W for the both modified polymers suggests an aggregation number of about 10−20, but in more concentrated solutions the apparent M_W of the aggregates indicates an aggregation number of only 2−3. These values are in agreement with the sequence observed for the R_h and R_g values. Moreover, the ratio R_g/R_h for modified polymers is much lower than that for the original dextran, in both the dilute and concentrated regime, suggesting the presence of more compact particles. For Dex-DCA polymer, this ratio is very close to the value of 0.775 expected for a compact sphere.

The change in the sign of the second virial coefficient between both concentration regimes in BAMDex solutions also indicates a change in the quality of the solvent (from good to bad solvent) due to the increase in the hydrophobically modified polymer concentration. Consequently, the increase in concentration of hydrophobically modified dextran, in fact the addition of more hydrophobic pendent groups to the medium, can be perceived as an increase in the fraction of a nonsolvent for the polymer.

In the transition concentration range, 0.02−0.2 g %, due to the change in the aggregate geometry, no reliable data could be obtained from the Zimm plots.

In Figure 9 the values of Kc/R_θ obtained from the extrapolation of eq 4 to $\theta = 0$ are plotted versus Dex-CA concentration. A clear slope change is observed for a polymer concentration $c_t \cong 0.30$ g %, indicating a change in the sign of A_2 and, consequently, a transition in the quality of the solvent. As the extrapolation of the two straight lines to $c = 0$ gives the value of $1/M_w$, the change from a good to a bad solvent is clearly accompanied by a decrease in the apparent M_w and transition from big and loose aggregates to small, very compact particles. A similar transition has been reported for xanthan−water solutions, but now resulting from the increase of temperature.[25] The driving force for this change is easily understandable and explained by the authors, but no such transition induced only by the increase in polymer concentration has been, to our knowledge, until now reported. A curious result from DLS and SLS measurements on dextran solubilized in water/dioxane mixtures is that, at low dioxane concentrations, dextran is better dissolved in the water/dioxane mixture than in water, but by increasing the dioxane concentration the R_g and A_2 values increase initially and then decrease.[33] This is in a way comparable with what we observe for BAMDexs in the case where we consider the hydrophobic substituent as a bad solvent for the modified polymer. Obviously, the CA and DCA are more than bad solvents, promoting aggregation probably due to specific interactions.

Conclusions

Both fluorescence and LS data show that BAMDexs form aggregates over the whole concentration range (0.001−2 g %) used in this study, but the size and shape of the aggregate are strongly dependent on the polymer concentration.

Below what we defined as the cac there is an initial critical concentration, c_i, at which isolated molecules begin to associate, forming big aggregates with a large number of polymer chains probably interacting through their hydrophobic groups. These loose aggregates are "swollen" with water, but the polarity of the medium inside them is lower than that of water. NPN, being hydrophobic, is trapped in these aggregates, partitioning between the dextran−water region and the aggregates of the cholic or deoxycholic moieties. An alternative explanation for the NPN fluorescence yield/fluorescence maximum behavior resides in the polydispersity of the polymer aggregates in this very low concentration range, if we accept that this polydispersity is reflected in the aggregate compactness and not only in the number of unimers per aggregate.

Table 2. Molecular Weight, Second Virial Coefficient, and Gyration Radius Obtained for Dextran and Hydrophobically Modified Dextrans from the Zimm Plots in the Low and High Concentration Ranges; the Hydrodynamic Radius from DLS and the Ratio R_g/R_h for the Same Polymers Are Also Included

	dextran		Dex-CA (DS = 4.0%)		Dex-DCA (DS = 3.6%)	
	0.002−0.020 g%	0.6−2.0 g%	0.002−0.020 g%	0.6−2.0 g%	0.002−0.020 g%	0.6−2.0 g%
mol wt (kg/mol)	32.6	39.9	720	58.4	852	78.5
2nd virial coeff (cm^3 mol/g^2)	$+3.0 \times 10^{-3}$	$+5.0 \times 10^{-3}$	$+5.7 \times 10^{-3}$	-1.7×10^{-4}	$+1.1 \times 10^{-3}$	-3.0×10^{-4}
radius of gyration, R_g (nm)	35	22.1	106	15.4	57	9.1
hydrodynamic radius, R_h (nm)	6	6	65	9.5	75	10
R_g/R_h	5.8	3.7	1.63	1.62	0.76	0.91

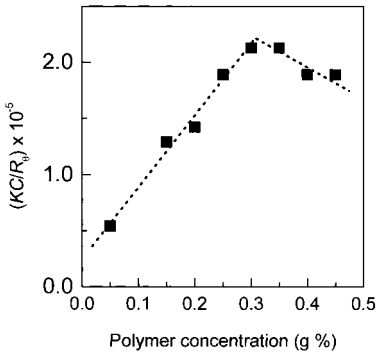

Figure 9. Scattered intensity extrapolated to zero angle versus concentration of Dex-CA (4.0 mol %) obtained from the SLS measurements on polymer solution with concentration in the range 0.05−0.5 g %.

The increase in polymer concentration above the cac induces the formation of more compact hydrophobic microdomains, as deduced from the increase in relative fluorescence intensity and decrease in hydrodynamic radius of polymer aggregate. A further increase in polymer concentration above a critical transition concentration, c_t, determines a transition of polymer chains from a random coil to a compact coil. This transition is accompanied by both a change in the quality of the solvent and the disruption of intermolecular associates, leading to small and very compact aggregates formed by only 2−3 polymer chains, with a high number of hydrophobic intra- and intermolecular junctions and a high local viscosity, in which a fluorescent probe like NPN partitions favorably.

These "critical concentrations" were observed for all the BAMDex studied here, but their values shift to lower values with the increase in the hydrophobicity of the pendent groups and degree of substitution.

The presence of large aggregates formed by intermolecular association at very low concentration has already been reported for other polymers, of both high and low molecular weight.[7,14,34] However, the transition from big to small aggregates with increase in concentration is very peculiar. The mechanism we suggest to explain this transition is based on the ability of bile acids to form micelles with very low aggregation numbers, the low molecular weight of polymers, and their low degree of substitution. For very dilute solutions the overall concentration of bile acid moiety is below its cmc, and the interaction between more than two bile acid moieties from the same polymer is less probable due to the relatively large persistence length of the dextran chain (5−10 units), the small degree of substitution, and the low polymer molecular weight (150 glucopyranosidic units). Consequently, no intrapolymer micelles can be formed despite the large local bile acid concentration. By contrary, a few hydrophobic junctions between several extended chains result in formation of bile acid micelles or, at least, long-lived aggregates. In the high concentration range we are probably above the bile acid moiety cmc, and aggregates of two or three polymer molecules allow the formation of micelles of at least four bile acid units. The occurrence of these micelles results in the aggregate shrinkage and their separation from the big and loose aggregates. This explanation obviously lacks experimental testing which might be obtained by comparing the cmc/cac of bile acids esterified with dextrans having different M_w, from small glucopyranosidic chains to very high molecular polysaccharides.

Acknowledgment. Authors are grateful to J. G. Martinho for many helpful discussions concerning the interpretation of LS data and use of the LS equipment. This work was supported in part by the program PRAXIS from FCT Portugal. M.N. is indebted to the Foundation for Science and Technology (FCT) of Portugal for grant PRAXIS XXI/BPD/14128/97.

References and Notes

(1) Glass, J. E., Eds. *Polymers in Aqueous Media: Performance through Association*; Advances in Chemistry 223; American Chemical Society: Washington, DC, 1989.
(2) Shalaby, S. W., McCormick, C. L., Butler, G. B., Eds. *Water Soluble Polymers*; ACS Symposium Series 467; American Chemical Society: Washington, DC, 1991.
(3) Dubin, P. J., Bock, J., Davis, R., Schulz, D. N., Thies, C., Eds. *Macromolecular Complexes in Chemistry and Biology*; Springer-Verlag: Berlin, 1994.
(4) Winnik, F. M. *J. Phys. Chem.* **1998**, *93*, 7452−7457.
(5) Biggs, S.; Selb, J.; Candau, F. *Langmuir* **1992**, *8*, 838−847.
(6) Morishima, Y.; Nomura, S.; Ikeda, T.; Seki, M.; Kamachi, M. *Macromolecules* **1995**, *28*, 2874−2881.
(7) Kramer, M. C.; Welch, C. G.; Steger, J. R.; McCormick, Ch. L. *Macromolecules* **1995**, *28*, 5248−5254.
(8) Hwang, F. S.; Hogen-Esch, T. E. *Macromolecules* **1995**, *28*, 3328−3335.
(9) Akiyoshi, K.; Deguchi, S.; Moriguchi, N.; Yamaguchi, S.; Sunamoto, J. *Macromolecules* **1993**, *26*, 3062−3068.
(10) Deguchi, S.; Akiyoshi, K.; Sunamoto, J. *Macromol. Rapid Commun.* **1994**, *15*, 705−711.
(11) Yusa, S.; Kamachi, M.; Morishima, Y. *Langmuir* **1998**, *14*, 6059−6067.
(12) Akiyoshi, K.; Deguchi, S.; Tajima, H.; Nishikawa, T.; Sunamoto, J. *Macromolecules* **1997**, *30*, 857−861.
(13) Lee, K. Y.; Jo, W. H.; Kwon, I. C.; Jeong, S. Y. *Macromolecules* **1998**, *31*, 378−383.
(14) Alami, E.; Rawiso, M.; Isel, F.; Beinert, G.; Binnana-Limbele, W.; François, J. In *Hydrophobic Polymers: Performance with Environmental Acceptability*; Glass, J. E., Ed.; Adv. Chem. Ser. 248; American Chemical Society: Washington, DC, 1996; pp 343−362.
(15) Alheim, M.; Hallensleben, M. L. *Makromol. Chem.* **1992**, *193*, 779−797.
(16) Walker, S.; Sofia, M. J.; Kakarla, R.; Kogan, N. A. *Proc. Natl. Acad. Sci. U.S.A.* **1996**, *93*, 1585−1590.
(17) Denike, J. K.; Zhu, X. X. *Macromol. Rapid Commun.* **1994**, *15*, 459−465.
(18) Brito, R. M. M.; Vaz, W. L. C. *Anal. Biochem.* **1986**, *152*, 250−255 and references therein.
(19) Lakowicz, J. R. *Principles of Fluorescence Spectroscopy*; Plenum Press: New York, 1983; p 113.
(20) Encinas, M. V.; Lissi, E. A. *Chem. Phys. Lett.* **1982**, *91*, 55−60.
(21) Zimm, B. H. *J. Chem. Phys.* **1948**, *16*, 1099−1116.

(22) Brown, W., Ed. *Light Scattering: Principle and Development*; Clarendon Press: Oxford, 1996.
(23) Kok, C. M.; Rudin, A. *Makromol. Chem., Rapid Commun.* **1981**, *2*, 655−659.
(24) Burchard, W. In *Laser Light Scattering in Biochemistry*; Harding, S. E., Sattelle, D. B., Bloomfield, V. A., Eds.; Royal Society of Chemistry: Cambridge, 1992; pp 3−22.
(25) Brant, D. A., Ed. *Solution Properties of Polysaccharides*; ACS Symposium Series 150; American Chemical Society: Washington, DC, 1981; p 8.
(26) Nichifor, M.; Carpov, A. *Eur. Polym. J.* **1999**, *35*, 2125−2129.
(27) Candau, F.; Regalado, E. J.; Selb, J. *Macromolecules* **1998**, *31*, 5550−5552.
(28) Azumi, T.; McGlynn, S. T. *J. Chem. Phys.* **1962**, *37*, 2413−2418.
(29) Maçanita, A. L.; Costa, F. P.; Costa, S. M. B.; Melo, E.; Santos, H. *J. Phys. Chem.* **1989**, *93*, 336−343.
(30) Glatter, O. In *Modern Aspects of Small-Angle Scattering*; Brumberger, H., Ed.; Kluwer Academic Publishers: Dordrecht, 1995; p 107.
(31) Lopes, A.; Maçanita, A.; Pina, F. S.; Melo, E.; Wamhoff, H. *Environ. Sci. Technol.* **1992**, *26*, 2448−2453.
(32) Picullel, L.; Thuresson, K., private communication.
(33) Sedlack, U.; Nordmeier, E. *Eur. Polym. J.* **1996**, *32*, 1109−1115.
(34) Marstokk, O.; Nyström, B.; Roots, J. *Macromolecules* **1998**, *31*, 4205−4212.

MA990408K